

**Thermal hysteresis of superparamagnetic Gd nanoparticle clusters**

C. M. Souza, S. S. Pedrosa, and A. S. Carriço\*

*Department of Physics, Universidade Federal do Rio Grande do Norte (UFRN), 59072-970 Natal, Rio Grande do Norte, Brazil*

G. O. G. Rebouças

*Department of Science and Technology, UFRSA, 59515-000 Angicos, Rio Grande do Norte, Brazil*

Ana L. Dantas†

*Department of Science and Technology, Universidade do Estado do Rio Grande do Norte (UERN), 59104-200 Natal, Rio Grande do Norte, Brazil*

(Received 8 April 2019; published 31 May 2019)

We report a theoretical study of the impact of dipolar interactions on the magnetic phases and thermal hysteresis of superparamagnetic Gd nanoparticle clusters. We consider Gd nanoparticles with size ranging from 5.5 to 10 nm, arranged with uniform density in a few-hundred-nanometer-sized ellipsoidal clusters. We show that in densely packed systems the dipolar interaction may grant thermal stabilization of the individual nanoparticle moments at high-temperature values, leading to large thermal loop widths, tunable by external magnetic fields of moderate strength. We have found, for instance, that with an external magnetic field strength of 85 Oe one may reach thermal loop widths ranging from 88 K for 5.5-nm-diam Gd nanoparticle clusters to 660 K for 8-nm-diam Gd nanoparticle clusters.

DOI: [10.1103/PhysRevB.99.174441](https://doi.org/10.1103/PhysRevB.99.174441)**I. INTRODUCTION**

Thermal hysteresis has been investigated in a number of nanostructured magnetic systems, including single-domain  $\text{Fe}_3\text{O}_4$  nanoparticles [1], alloys [2], multilayers [3–6], thin rare-earth films [7,8], ferromagnetic (FM) nanoparticles exchange coupled to antiferromagnetic (AFM) substrates [9], and FM/AFM bilayers [10].

The thermal hysteresis in these magnetic systems is attractive because the thermal loop widths may reach a few hundred degrees Kelvin. Furthermore, the thermal loop widths are tunable by external magnetic fields of modest magnitude, and reveal the new magnetic phases due to confinement effects and contact interaction of thin films and nanostructured multilayered systems [4,7,8].

In this paper, we discuss the impact of the dipolar interaction on the magnetic phases and the magnetic thermal hysteresis of ellipsoidal clusters comprising densely packed Gd nanoparticles with size ranging from 5.5 to 10 nm.

We have selected Gd nanoparticle clusters so that the dipolar interaction between the particles has the prominent role in the magnetic phases. The Gd nanoparticles have large magnetization and rather small magnetic anisotropy for temperatures above 200 K [11]. Furthermore, we assume there is no exchange interaction between the nanoparticles, and the magnetic phases of the Gd nanoparticle clusters are entirely controlled by the nanoparticle dipolar interactions. Thus, the magnetic phases may be efficiently tailored by the values of

the nanoparticle diameters, the cluster size and topological layout, the nanoparticle packing density, and the external magnetic field strength.

In densely packed magnetic nanoparticle clusters, a relevant number of nanoparticles may be within the reach of the dipolar field of most of the other nanoparticles. In this case, the nanoparticle dipolar interactions may stabilize the magnetic order and the nanoparticle cluster may exhibit collective behavior [12,13] and superferromagnetism [14,15].

The dipolar interaction is long ranged and anisotropic, and the dipolar sums are affected in a relevant manner by the relative positions of the nanoparticles in the cluster. Thus, the impact of the dipolar interaction on the cluster magnetic phases is likely to be strongly affected by the cluster topology, which controls the global nanoparticle positioning within the cluster, as well as the structure of the lattice containing the nanoparticles [16].

For applications, a random distribution of nanoparticle distances, disorder in the nanoparticle positioning, or random distribution of the nanoparticle sizes may lead to the formation of superspin-glass phases [17–19]. The large degeneracy of the superspin-glass phases may turn into a serious obstacle for applications. Nearly uniform systems, with the nanoparticles in periodical lattices, are required to designing systems with better chances of having reproducible magnetic properties. Furthermore, uniform Gd nanoparticle clusters, with a periodical nanoparticle positioning, allow not only the selection of key magnetic phases but also the control of sharp transitions between these magnetic phases, as we discuss in the present paper.

We have recently shown [16] that the dipolar interaction between nanoparticles leads to the formation of the dipolar

\*ascarrico@gmail.com

†dantasal@gmail.com

spin-flop state (DSFS), the vortical state (VS), and the antiferromagnetic state (AFS) along the room-temperature magnetic hysteresis curves of ellipsoidal clusters of superparamagnetic  $\text{Fe}_3\text{O}_4$  nanoparticles, for external magnetic fields applied along the major axis direction.

In our recent results [16], the vortical state was found in the room-temperature magnetic hysteresis loop of spherical clusters and low-eccentricity ellipsoidal clusters of superparamagnetic nanoparticles. However, for high-eccentricity ellipsoidal clusters, the vortical state is not formed at the room-temperature magnetic hysteresis curve. In this eccentricity limit we have found only the DSFS and AFS, apart from the uniform magnetic phase, along the room-temperature hysteresis curves.

We have discussed the impact of the interparticle dipolar interaction on the magnetic phases and reproduced [16] the main features of previous experimental results, either reporting susceptibility enhancement or dipolar ferromagnetism in large-nanoparticle-packing-density Fe and Co linear chains [20,21]. We have also reproduced experimental results reporting the reduction of the initial susceptibility of spherical clusters of  $\text{Fe}_3\text{O}_4$  superparamagnetic nanoparticles [22,23].

In this paper, we discuss thermal hysteresis effects of Gd nanoparticle clusters. We show that, using external magnetic fields of moderate strength, high-eccentricity ellipsoidal clusters of densely packed superparamagnetic Gd nanoparticles may exhibit large thermal loop widths.

The thermal hysteresis is due to transitions between the DSFS and the AFS of the Gd nanoparticle clusters. We have found that the DSFS may be formed at high temperatures, with a partial alignment of the magnetic moments with the external magnetic field. The AFS forms at lower temperatures with the magnetic moments aligned with the dipolar field.

Along the cooling and the heating branches of the thermal loop, there is a transition from one state to the other, but the transition temperature depends on the external field strength and whether one is heating or cooling. This difference in transition temperatures originates the thermal hysteresis.

## II. THEORETICAL MODEL

We consider high-eccentricity three-dimensional ellipsoidal clusters holding Gd superparamagnetic nanoparticles confined with uniform density. The nanoparticles are located on the sites of simple cubic lattices, and the lattice parameter is adjusted to set the nanoparticle packing density.

In Fig. 1 we show a schematic representation of an  $xy$ -plane cross section of an ellipsoidal cluster of superparamagnetic Gd nanoparticles showing the semimajor and semiminor axes ( $a$  and  $b$ ). The major axis is along the  $x$ -axis direction. The spherical Gd nanoparticles have diameter  $D$  and are distributed uniformly with a center-to-center distance  $d$ .

The cluster equilibrium magnetic phases are found using local-field algorithms which allow calculating the orientations and the thermal average values of the nanoparticle magnetic moments ( $\langle \vec{\mu}_j \rangle$ ,  $j = 1, \dots, N$ ) in a self-consistent manner. The nanoparticle moment orientations and thermal average values are adjusted self-consistently to satisfy the equilibrium conditions taking into account the features associated with the long-ranged and anisotropic nature of the dipolar interaction.

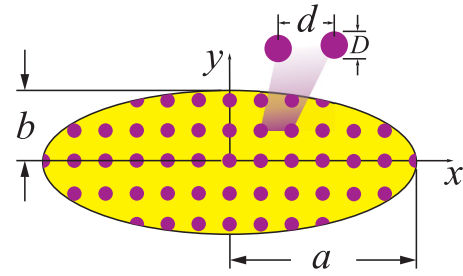


FIG. 1. A schematic representation of an  $xy$ -plane cross section of an ellipsoidal cluster of superparamagnetic Gd nanoparticles showing the semimajor and semiminor axes ( $a$  and  $b$ ). The spherical nanoparticles have diameter  $D$  and are distributed uniformly with a center-to-center distance  $d$ .

We consider the dipolar sums in full, with no restrictions on the number of terms. Therefore, the equilibrium values of the orientation and the thermal average value of the magnetic moment of any one of the Gd nanoparticles are related globally with the magnetic phase of the cluster.

The effective local field at each nanoparticle is obtained from the magnetic energy,  $\vec{H}_j^{\text{eff}} = -\partial E / \partial \vec{\mu}_j$ , and the thermal average values are calculated using a Langevin average for each nanoparticle,  $\langle \vec{\mu}_j \rangle = \mu_0 \mathcal{L}(\mu_0 H_j^{\text{eff}} / k_B T) \hat{\mu}_j$ , where  $\mu_0$  is the saturation value of the nanoparticle magnetic moment,  $\hat{\mu}_j$  is the unit vector in the direction of the thermal average magnetic moment, and  $\mathcal{L}$  is the Langevin function ( $\mathcal{L}(x) = \coth(x) - 1/x$ ).

The equilibrium configuration conditions are found by adjusting self-consistently the nanoparticle magnetic moment directions and thermal values to having each nanoparticle magnetic moment aligned with the effective local field, so that the magnetic torque acting on each nanoparticle is zero ( $\langle \vec{\mu}_j \rangle \times \vec{H}_j^{\text{eff}} = 0$ ,  $j = 1, \dots, N$ ). Convergence is checked to ensure that the magnetic torque in any one of the nanoparticles is smaller than  $10^{-29}$  J.

The magnetic energy is given by

$$E = - \sum_{j=1}^N \vec{H} \cdot \vec{\mu}_j + \frac{1}{2} \sum_{j=1}^N \sum_{k=1}^N \times \left( \frac{\vec{\mu}_j \cdot \vec{\mu}_k}{R_{jk}^3} - \frac{3(\vec{\mu}_j \cdot \vec{R}_{jk})(\vec{\mu}_k \cdot \vec{R}_{jk})}{R_{jk}^5} \right), \quad (1)$$

where the first term is the Zeeman energy, and in the dipolar energy term the vector  $\vec{R}_{jk}$  is the relative position of the Gd nanoparticles with magnetic moments  $\vec{\mu}_j$  and  $\vec{\mu}_k$ ,  $N$  is the number of Gd nanoparticles, and the sum over  $k$  is restricted to  $k \neq j$ . We have used the bulk value of the Gd magnetization parameter [24],  $M = 2.117$  kG.

We have found that for a given cluster there are two temperature regimes. The first regime is the very-high-temperature regime, in which the thermal average magnetic moments of the nanoparticles are too small, so that the dipolar field produced by the nanoparticles is much smaller than the external magnetic field strength.

The second regime is the moderate-temperature regime and corresponds to values of the temperature for which the magnitude of the dipolar field produced by the nanoparticles

is comparable to, or larger than, the external magnetic field strength.

We consider thermal loops, within the temperature interval from 200 to 1200 K, in the presence of an external magnetic field  $H$ , of moderate strength, and parallel to the long axis of the ellipsoidal cluster.

The thermal loops consist of a cooling branch, starting at a temperature value in the very-high-temperature regime, and extending down to a small-temperature value, smaller than that required for the DSFS-AFS transition, in the moderate-temperature regime, followed by the heating branch, covering the same temperature interval.

The sequence of magnetic phases along the cooling branch of the thermal loop is calculated by starting at a temperature value within the very-high-temperature regime. At this temperature we initialize the self-consistent equations by using the aligned state (AS) as the initial guess, with all the magnetic moments in the direction of the external field, with a thermal average value equal to a rather small fraction of the saturation value ( $\langle \mu_j \rangle / \mu_0 \ll 1.0$ ). Solving the self-consistent equations we determine the equilibrium values of the nanoparticle moment orientations and thermal average values of the magnetic moments.

The equilibrium magnetic phase ( $\langle \vec{\mu}_j \rangle$ ,  $j = 1, \dots, N$ ) at a given temperature is then used as the initial guess to the next temperature value, along the cooling branch.

The sequence of magnetic phases in the heating branch is calculated similarly, starting with the magnetic phase corresponding to the lowest temperature of the cooling branch.

### III. RESULTS AND DISCUSSIONS

#### A. General remarks

The central element for the thermal hysteresis of Gd superparamagnetic nanoparticle clusters is the effect of the large dipolar field produced by the cluster itself in the thermal stabilization of the Gd nanoparticle magnetic phases.

The transition temperatures in both branches of the thermal loop depend on the dipolar field and the external magnetic field strengths. We have found that increasing the Gd nanoparticle diameter, or the nanoparticle packing density, leads to stronger dipolar effects and larger thermal loop widths.

As shown in Table I, we have found, for instance, that for an external magnetic field strength of 85 Oe, and densities of the order of  $10^3$  Gd nanoparticles/cm<sup>3</sup>, 8-nm-diam Gd clusters display a 660 K thermal hysteresis loop width, which is much larger than the corresponding thermal hysteresis loop width of 88 K of 5.5-nm-diam Gd nanoparticle clusters.

We note that the dipolar interaction is an essential ingredient for the existence of thermal hysteresis. Without it, each nanoparticle would be subjected solely to the external field. In this case all the Gd nanoparticles in the cluster would be equivalent and would have a thermal average magnetic moment along the external field direction. The average magnetic moment of any of the Gd nanoparticles in the cluster would be the same, and given by the Langevin function  $\mathcal{L}(x)$ , with  $x = \mu_0 H / k_B T$ , where  $H$  is the strength of the external field and  $\mu_0$  is the saturation value of the magnetic moment of the Gd nanoparticle. No thermal hysteresis would be possible. Thus,

TABLE I. External field effects on the thermal hysteresis loop width  $\delta T$  of ellipsoidal clusters with 5.5-, 8-, and 10-nm-diam Gd nanoparticles distributed uniformly, with center-to-center nanoparticle distances of 10.2, 14.4, and 22 nm (see text for details of the clusters dimensions).  $T_1$  and  $T_2$  are the temperatures for the DSFS-AFS transition in the cooling branch and the AFS-DSFS transition in the heating branch, respectively.

$D$ (nm)	$H$ (Oe)	$T_1$ (K)	$T_2$ (K)	$\delta T$ (K)
5.5	81	272	355	83
	85	259	347	88
	87	248	342	94
8.0	91	224	334	110
	81	560	1150	590
	83	470	1080	610
	85	370	1030	660
10.0	88	230	980	750
	45	540	1190	650
	46	452	1134	682
	47	364	1090	726
	48.5	210	1046	836

we stress that the existence of thermal hysteresis is a signature of the dipolar interaction between the Gd nanoparticles.

We have shown recently that the dipolar interaction favors the nucleation of the AFS in high-eccentricity ellipsoidal clusters of superparamagnetic Fe<sub>3</sub>O<sub>4</sub> nanoparticles [16]. In remanence, the AFS may display a nearly full thermal value of the nanoparticle magnetic moments and large values of the dipolar field strength [16].

The nucleation of the AFS induced by the large values of the Gd nanoparticle cluster dipolar field strength at low temperature values is a key feature of the thermal hysteresis loops of Gd superparamagnetic nanoparticle clusters.

Furthermore, we have found that the dipolar interaction may lead to surprisingly large thermal average values of the nanoparticle's magnetic moments. For instance, above room temperature, the average dipolar field strength may reach a few hundred oersted and stabilize the magnetic moment values to large fractions of the saturation value.

Also, in the cooling branch of the thermal loop, modest changes in the external magnetic field strength may lead to significant variations in the value of the temperature for the DSFS-to-AFS transition, favoring the control of the thermal loop width by the external magnetic field.

The Zeeman energy demands magnetization along the external field direction, as in the DSFS. The dipolar energy is favored in the AFS, and the dipolar interaction turns stronger as the temperature is reduced. Thus, as shown in cooling branch curves in Fig. 2, if the external field strength increases, a lower value of the temperature is required to allow the transition from the DSFS to the AFS.

In Fig. 2 we show the magnetization curves along the cooling branches of a 1017-nm-long axis and 0.97-eccentricity ellipsoidal cluster holding 1671 Gd nanoparticles with 10 nm diameter, distributed with a center-to-center distance of 26.5 nm.

Notice that there is a considerable variation of the value of the temperature for the DSFS-to-AFS transition, for small

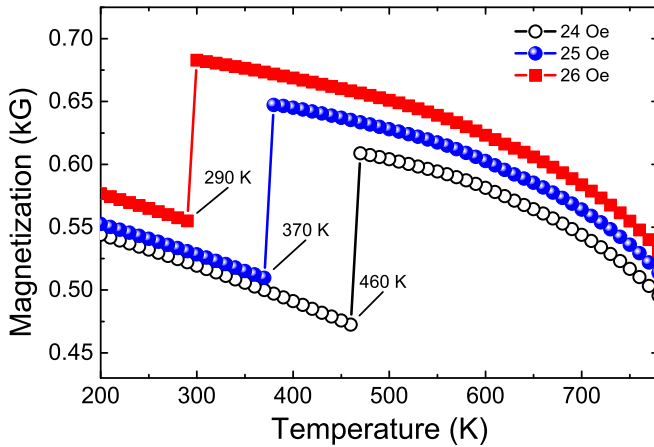


FIG. 2. Magnetization curves along the cooling branches of a 1017-nm-long axis and 0.97-eccentricity ellipsoidal cluster of 10-nm-diam Gd nanoparticles distributed with a center-to-center distance of 26.5 nm, for external magnetic field strengths of 24, 25, and 26 Oe. The transitions from the DSFS to the AFS occur at temperatures of 460, 370, and 290 K.

changes in the external field strength. The curves correspond to external magnetic field strengths of 24, 25, and 26 Oe and show the transition from the DSFS to the AFS at temperatures of 460, 370, and 290 K.

In Figs. 3 and 4 and throughout the paper, the panels show the Gd nanoparticle magnetic moment patterns, and the dipolar field patterns in the cluster  $z = 0$  layer. A pair of panels is associated with each temperature. In the upper

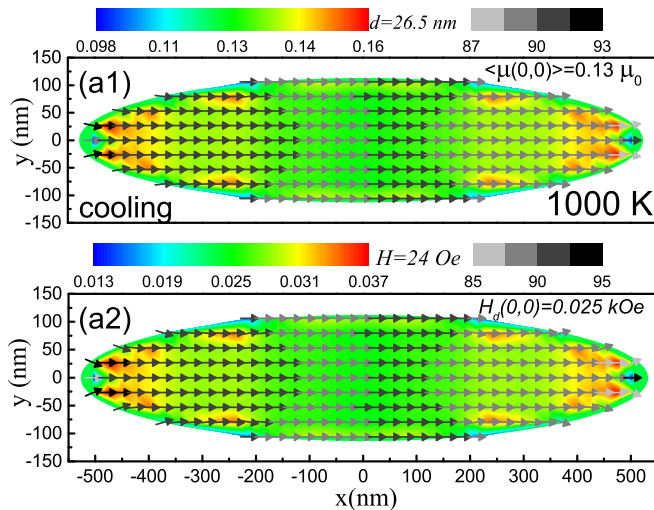


FIG. 3. (a1) Thermal average magnetic moment ( $\langle \mu \rangle / \mu_0$ ) and (a2) dipolar field patterns at 1000 K, corresponding to an external field strength of 24 Oe, in the cooling branch of the 10-nm-diam Gd cluster shown in Fig. 2. The left-hand-side color bars shows either (a1) the values of the fractional thermal average magnetic moment per Gd nanoparticle or (a2) the strength of the dipolar field in units of kOe. The right-hand-side color bars show the out-of-plane angles ( $\theta$ ) of the nanoparticle magnetic moments or the dipolar field. The values of the magnetic moment ( $\langle \mu(0, 0) \rangle$ ) and the dipolar field strength ( $H_d(0, 0)$ ), at the cluster center, are also given in each panel.

(lower) panels we show the magnetization (dipolar field) patterns. The left-hand-side color bars show either the values of the fractional thermal average magnetic moment per nanoparticle  $\langle \mu / \mu_0 \rangle = \langle \mu \rangle / \mu_0$ , where  $\mu_0$  is the saturation magnetic moment and  $\langle \mu \rangle$  is the thermal average magnetic moment of the Gd nanoparticle, or the strength of the dipolar field in units of kOe. The out-of-plane angle ( $\theta$ ) is the angle with the  $z$  axis, and  $\phi$  is the angle with the  $x$  axis.

For  $H = 24$  Oe, we have found that at a temperature of 1000 K the thermal average dipolar field is around 25 Oe and the thermal average value of the nanoparticle magnetic moments is around 10% of the saturation value ( $\langle \mu \rangle \approx 0.13\mu_0$ ), as shown in Figs. 3(a1) and 3(a2).

At a temperature of 780 K the DSFS forms. As shown in Figs. 4(a1) and 4(a2) the thermal average values of the dipolar field and the nanoparticle moments increase to 92 Oe and  $0.33\mu_0$ . The DSFS covers a small fraction of the magnetic moments at the cluster center. Away from the cluster center the thermal average values of the magnetic moments and dipolar field are reduced to  $\langle \mu \rangle \approx 0.2\mu_0$  and  $H_d \approx 50$  Oe.

By further reducing the temperature, the AFS forms at 460 K. In the AFS at 460 K, as shown in Figs. 4(b1) and 4(b2), a significant fraction of the Gd nanoparticles has large values of the thermal average magnetic moment and dipolar field:  $\langle \mu \rangle \approx 0.76\mu_0$  and  $H_d \approx 0.258$  kOe. Notice that in the AFS the thermal average dipolar field produced by the Gd nanoparticles is more than ten times larger than the external field strength.

The thermal hysteresis phenomenology can be understood as follows. The local field at each Gd nanoparticle sums the external field and the dipolar field produced by the other Gd nanoparticles. The dipolar field produced by each Gd nanoparticle is proportional to the thermal average value of its magnetic moment. As the temperature is reduced the thermal average value of the magnetic moment of each Gd nanoparticle increases. Thus, the strength of the dipolar field produced by the cluster increases as the temperature is reduced.

Starting the cooling branch at very high temperatures, in the presence of an external magnetic field of modest intensity, each nanoparticle acquires a rather small fraction of its magnetic moment and produces a rather weak dipolar field. Thus, the magnetic field acting on each nanoparticle is along the external field direction. The cluster is in the AS, with the magnetic moment of each nanoparticle aligned with the direction of the external field.

By reducing the temperature, along the cooling branch, at some temperature value, the thermal average values of the nanoparticle moments are no longer small, and the dipolar field in the cluster is not negligible. The local field acting on each one of the nanoparticles is no longer in the direction of the external field. Instead, the dipolar field and the nanoparticle magnetic moments adjust to each other. At this temperature, the DSFS is formed.

For low-temperature values, the dipolar field strength in the cluster may turn out to be much larger than that of the external magnetic field. In this case, the magnetic field acting on all nanoparticles in the cluster is nearly equal to the dipolar field produced by the cluster itself. The magnetic moments of all nanoparticles turn parallel to the dipolar field, and the cluster magnetic phase tends to replicate the dipolar field pattern.

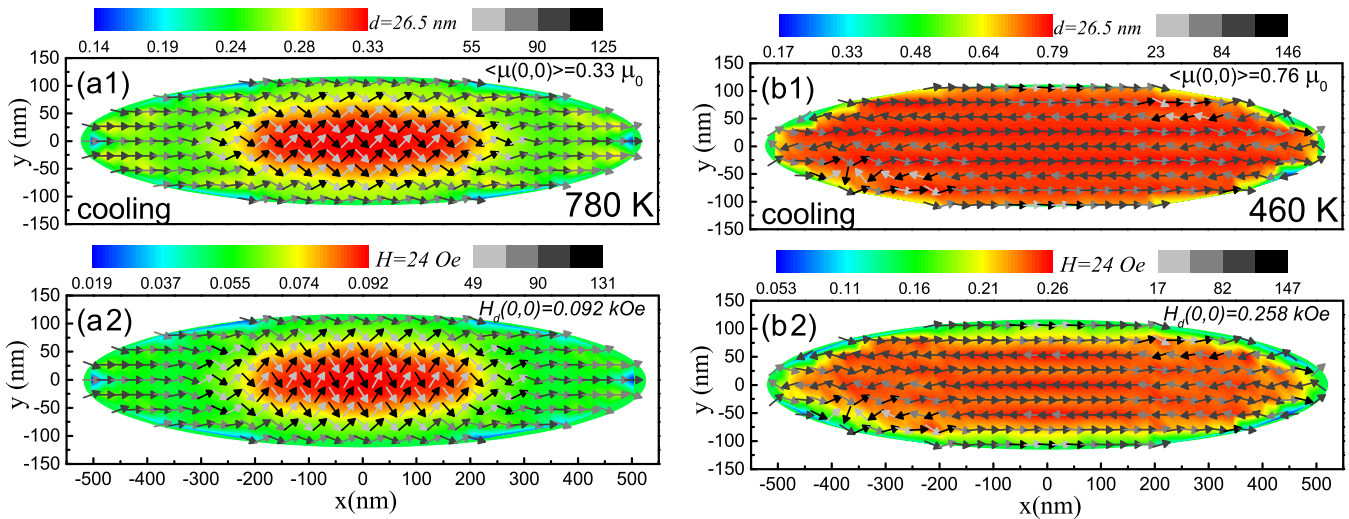


FIG. 4. (a1) Thermal average magnetic moment ( $\langle \mu \rangle / \mu_0$ ) and (a2) dipolar field patterns of a 1017-nm-long axis and 0.97-eccentricity ellipsoidal cluster of 10-nm-diam Gd nanoparticles distributed with a center-to-center distance of 26.5 nm, for an external magnetic field strength of 24 Oe and a temperature of 780 K. In (b1) and (b2) we show the corresponding values for a temperature of 460 K. The left-hand-side color bars show either the values of the fractional thermal average magnetic moment per Gd nanoparticle, or the strength of the dipolar field in units of kOe. The right-hand-side color bars show the out-of-plane angles ( $\theta$ ) of the nanoparticle magnetic moments or the dipolar field. The values of the magnetic moment ( $\langle \mu(0, 0) \rangle$ ) and the dipolar field strength ( $H_d(0, 0)$ ), at the cluster center, are also given in each panel.

Throughout the paper, we use  $T_1$  for the temperature for the transition from the DSFS to the AFS in the cooling branch of the thermal loop and  $T_2$  for the temperature for the transition from the AFS to the DSFS in the heating branch.

Starting at the nucleation of the DSFS, by reducing the temperature, the individual nanoparticle magnetic moments align progressively with the local dipolar field.

The gradual alignment with the dipolar field leads to enhancement of the thermal average values of the Gd nanoparticle magnetic moments and the intensity of the dipolar field, favoring the transition to the AFS at a temperature  $T_1$ . By further reducing the temperature, the thermal average values of the magnetic moments and dipolar field increase, leading to extra stability of the AFS.

The cluster exhibits thermal hysteresis if along the heating branch, starting in the AFS at low temperatures, the AFS stays stable up to a temperature  $T_2$ , larger than  $T_1$ . This may be achieved by properly choosing the Gd nanoparticle diameter, the nanoparticle packing density, the cluster size and eccentricity, and the external magnetic field strength as shown in Table I. The thermal loop width is given by  $\delta T = T_2 - T_1$ .

### B. 5.5-nm-diam Gd nanoparticle cluster

We show the thermal hysteresis loop of a 310.75-nm major axis and 66.55-nm minor axis ellipsoidal Gd nanoparticle cluster for an external field of 85 Oe in Fig. 5. The cluster holds 795 Gd nanoparticles with 5.5 nm diameter distributed uniformly, with a center-to-center distance of 10.2 nm.

In Fig. 5 the thermal cycle begins above room temperature, at  $T = 400$  K. The Gd superparamagnetic cluster is cooled down to a temperature of 225 K and then heated back to a temperature of 400 K. As shown in Fig. 5, the thermal hysteresis has a loop width of  $\delta T = 88$  K around room temperature, extending from  $T_1 = 259$  to  $T_2 = 347$  K.

In Fig. 6 we show details of the magnetic phases for selected points in the cooling and heating branches of the thermal loop shown in Fig. 5. As shown in Fig. 6 the sequences of magnetic phases along the cooling and heating branches are different.

The cooling branch starts at 400 K with the cluster in the AS. As shown in Fig. 6(a) all the Gd nanoparticle magnetic moments are aligned with the external field direction. The magnetization and dipolar field patterns are shown in Figs. 6(a1) and 6(a2). The thermal averages of the magnetic moments, as shown in Fig. 6(a1), and dipolar field strength, as shown in Fig. 6(a2), are around  $\langle \mu \rangle \approx 0.25 \mu_0$  and

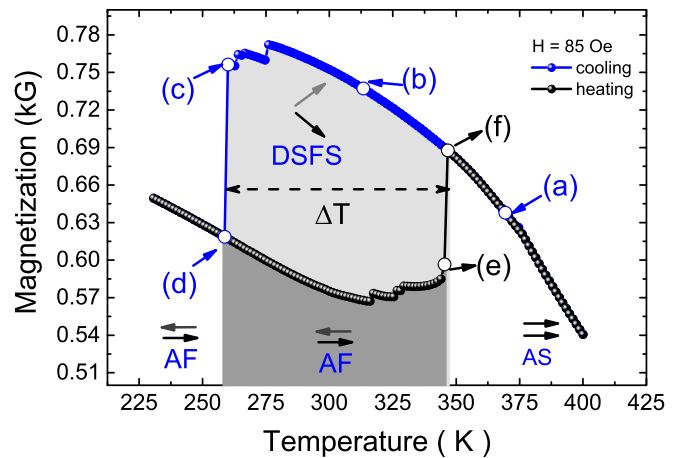


FIG. 5. Thermal hysteresis loop of a 310.75-nm major axis and 66.55-nm minor axis ellipsoidal cluster of 5.5-nm-diam Gd nanoparticles. The cluster holds 795 Gd nanoparticles distributed uniformly, with a center-to-center distance of 10.2 nm, and the external field strength is 85 Oe.

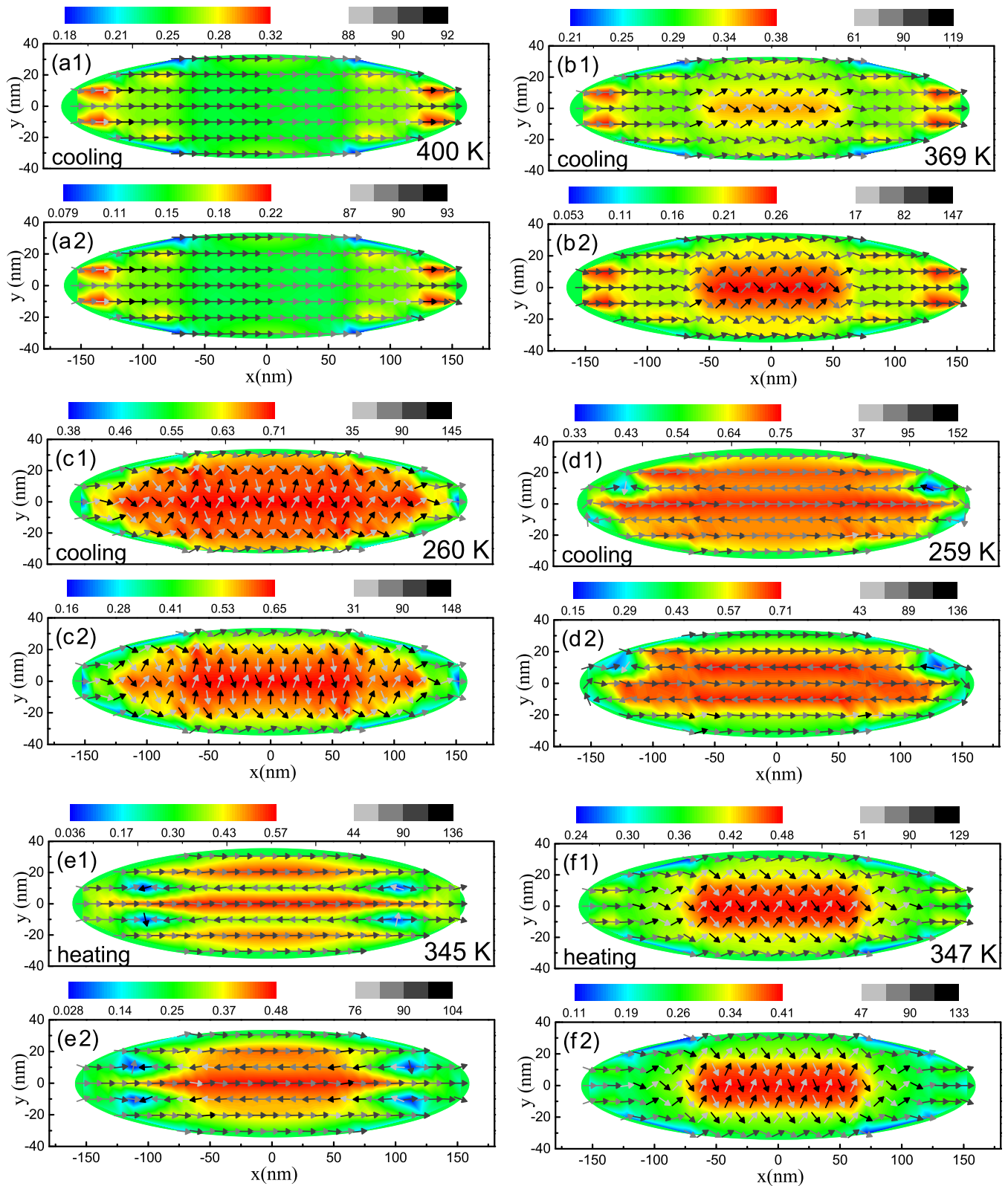


FIG. 6. Thermal average magnetic moment ( $\langle\mu\rangle/\mu_0$ ) (upper panels) and dipolar field patterns (lower panels) for selected temperature values as indicated in Fig. 5, in the cooling or the heating branch of the thermal hysteresis loop for a 310.75-nm major axis and 66.55-nm minor axis ellipsoidal clusters of 5.5-nm-diam Gd nanoparticles distributed uniformly, with a center-to-center distance of 10.2 nm. The left-hand-side color bars show either the values of the fractional thermal average magnetic moment per Gd nanoparticle, or the strength of the dipolar field in units of kOe. The right-hand-side color bars show the out-of-plane angles ( $\theta$ ) of the Gd nanoparticle magnetic moments or the dipolar field.

$H_d \approx 0.15$  kOe. Notice that the dipolar field strength is almost twice as large as the external field strength.

The DSFS forms at a temperature of 369 K. As shown in Figs. 6(b1) and 6(b2), the DSFS forms in the central part of the cluster where the thermal average magnetic moments and dipolar field values are around  $\langle \mu \rangle \approx 0.35\mu_0$  and  $H_d \approx 0.26$  kOe.

The DSFS spreads over progressively larger fractions of the nanoparticles as the temperature is reduced. At 260 K, as shown in Figs. 6(c1) and 6(c2), the DSFS covers most of the cluster. The magnetic moments and dipolar field values are around  $\langle \mu \rangle \approx 0.71\mu_0$  and  $H_d \approx 0.649$  kOe at the cluster center and most of the nanoparticles except near the cluster magnetic poles.

At 259 K the AFS is nucleated with slightly larger values of the magnetic moments and dipolar field. The thermal average values of the magnetic moments and dipolar field are around  $\langle \mu \rangle \approx 0.73\mu_0$  and  $H_d \approx 0.69$  kOe at the cluster center, as shown in Figs. 6(d1) and 6(d2).

By further cooling, the AFS stays stable down to 225 K. Along the heating branch the AFS stays stable till 345 K, as shown in Figs. 6(e1) and 6(e2), and the thermal loop closes at 347 K, with the transition back to the DSFS, as shown in Figs. 6(f1) and 6(f2).

As shown in Table I, both  $T_1$  and  $T_2$  are decreasing functions of the external field strength.  $T_1$  and  $T_2$  vary from 272 and 355 K, respectively, down to 224 and 334 K, as the external field strength is changed from 81 to 91 Oe. The reduction in  $T_1$  is larger and the thermal loop width varies between 83 and 110 K for a 10-Oe increase in the external field strength.

We have also found that for large values of the external field strength there is no thermal hysteresis, because the Zeeman energy inhibits the formation of the AFS. For instance, for an external field strength of 100 Oe the DSFS forms at 363 K, in the cooling branch, and stays stable down to low-temperature values, around 200 K. In this case, the sequence of states in the heating branch curve is equal to that in the cooling branch curve. This might be a point of some interest for applications of superparamagnetic clusters.

### C. 8.0-nm-diam- Gd nanoparticle cluster

In Fig. 7 we show the thermal hysteresis loop of an 8-nm-diam Gd nanoparticle ellipsoidal cluster, with a 555-nm major axis and a 123-nm minor axis. The cluster holds 1671 Gd nanoparticles distributed uniformly with a center-to-center distance of 14.4 nm, and the external field strength is 88 Oe.

In Table I we show the external field dependence of the thermal loop width of the 8-nm-diam Gd cluster. As shown, for similar values of the external field strengths, the thermal loop widths are much larger than the corresponding loop width for the 5.5-nm-diam Gd cluster.

A comparison of the data in Table I reveals much larger dipolar effects in the thermal hysteresis of the 8-nm-diam Gd cluster. For instance, for an external field strength of 81 Oe, the values of the DSFS-AFS transition temperature, and the thermal loop width, for the 5.5-nm-diam Gd nanoparticle cluster are  $T_1 = 272$  K,  $T_2 = 355$  K,

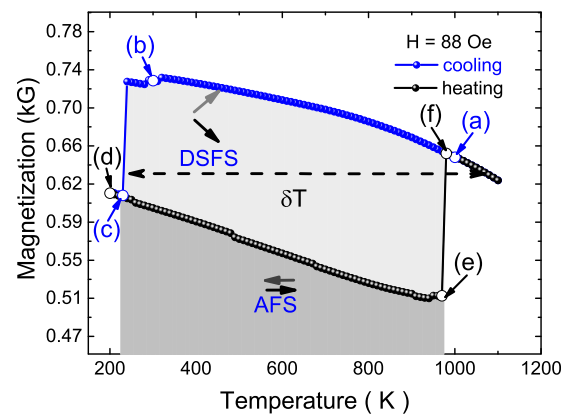


FIG. 7. Thermal hysteresis loop of an 8-nm-diam Gd cluster, with a 555-nm major axis and a 123-nm minor axis. The cluster holds 1671 Gd nanoparticles distributed uniformly with a center-to-center distance of 14.4 nm and the external field strength is 88 Oe.

and  $\delta T = 83$  K. The corresponding values for the 8-nm-diam Gd nanoparticle cluster are  $T_1 = 560$  K,  $T_2 = 1150$  K, and  $\delta T = 590$  K.

In Fig. 8 we show details of the magnetic phases along selected temperature values, as indicated in Fig. 7, in the cooling and the heating branches of the 8-nm-diam Gd cluster, for an external field strength of  $H = 88$  Oe.

Notice that the magnetic phases reveal that the dipolar effects are much stronger in the 8-nm-diam Gd cluster. For instance, as shown in Figs. 8(a1) and 8(a2), at a temperature of 1000 K the DSFS is already formed. Furthermore, the thermal average values of the Gd nanoparticle magnetic moments and the dipolar field in the cluster are large: they are around  $\langle \mu \rangle \approx 0.63\mu_0$  and  $H_d \approx 0.62$  kOe.

In the 5.5-nm-diam Gd cluster, for an external field strength of 85 Oe the nucleation of the DSFS requires a much lower temperature value of 369 K. Furthermore, as shown in Figs. 6(b1) and 6(b2), the corresponding values of the thermal average values of the Gd nanoparticle magnetic moments and the dipolar field are around  $\langle \mu \rangle \approx 0.35\mu_0$  and  $H_d \approx 0.26$  kOe. Thus, the DSFS of the 5.5-nm-diam Gd cluster is formed at a lower temperature, but the thermal average values of the Gd nanoparticle magnetic moments and the dipolar field in the cluster are smaller than the corresponding values of the 8-nm-diam Gd cluster in the DSFS at 1000 K.

As shown in Figs. 8(b1) and 8(b2), at room temperature the magnetic moments in the DSFS are near saturation with thermal average values around  $\langle \mu \rangle \approx 0.92\mu_0$ , with a corresponding large value of the cluster dipolar field, which is around  $H_d \approx 0.9$  kOe.

The AFS is formed at  $T_1 = 230$  K with the magnetic moment thermal average values around  $\langle \mu \rangle \approx 0.94\mu_0$  and the thermal average dipolar field is around  $H_d \approx 1.0$  kOe, as shown in Figs. 8(c1) and 8(c2), and stays stable to 200 K with the magnetic moment thermal average values around  $\langle \mu \rangle \approx 0.95\mu_0$  and the thermal average dipolar field is around  $H_d \approx 1.0$  kOe, as shown in Figs. 8(d1) and 8(d2).

In the heating branch, the AFS stays stable from 200 K to high-temperature values. As shown in Figs. 8(e1) and 8(e2), at 970 K the AFS is confined to the ellipsoid central region, with

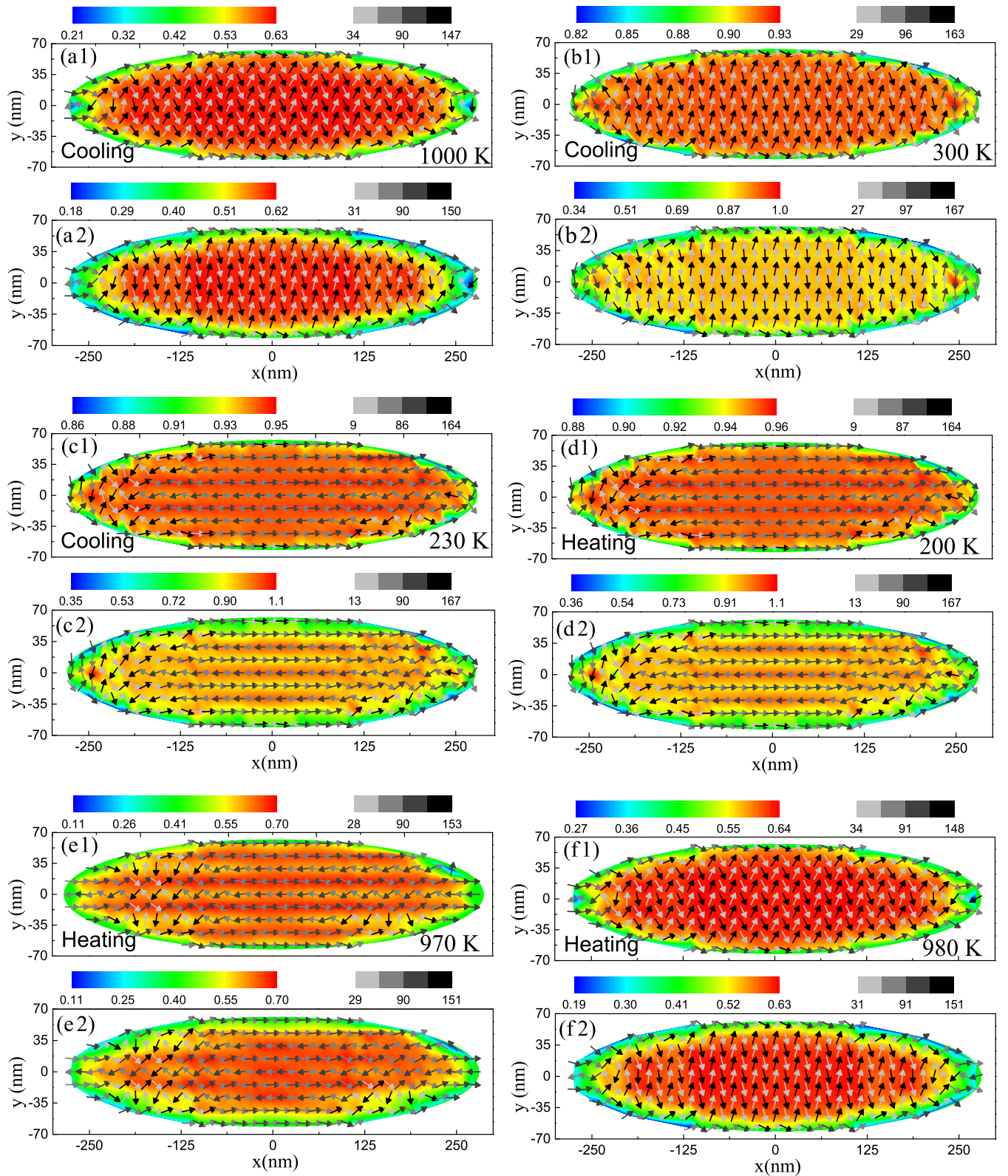


FIG. 8. Thermal average magnetic moment ( $\langle\mu\rangle/\mu_0$ ) (upper panels) and dipolar field patterns (lower panels) for selected temperature values, as indicated in Fig. 7, in the cooling or the heating branch of the thermal hysteresis loop for 555-nm major axis and 123-nm minor axis ellipsoidal clusters holding 1671 Gd nanoparticles, with 8 nm diameter, distributed uniformly with a center-to-center distance of 14.4 nm. The left-hand-side color bars show either the values of the fractional thermal average magnetic moment per Gd nanoparticle, or the strength of the dipolar field in units of kOe. The right-hand-side color bars show the out-of-plane angles ( $\theta$ ) of the nanoparticle magnetic moments or the dipolar field.



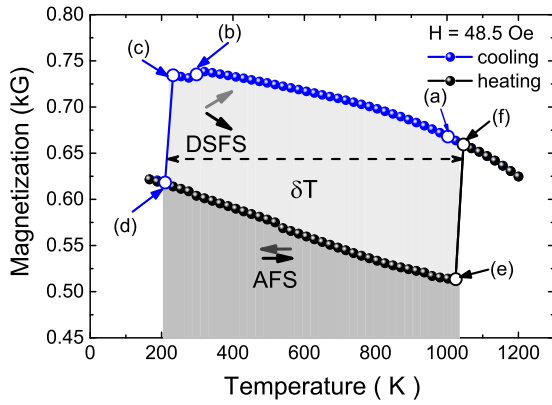


FIG. 9. Thermal hysteresis loop of a 10-nm-diam Gd cluster, with an 846-nm major axis and a 186-nm minor axis. The cluster holds 1671 Gd nanoparticles distributed uniformly with a center-to-center distance of 22.0 nm and the external field strength is 48.5 Oe.

the magnetic moment thermal average values around  $\langle \mu \rangle \approx 0.70\mu_0$  and the thermal average dipolar field around  $H_d \approx 0.7$  kOe. The transition to the DSFS occurs at  $T_2 = 980$  K, as shown in Figs. 8(f1) and 8(f2), leading to a thermal loop width of  $\delta T = 750$  K.

One might argue that, because it has a center-to-center distance of 14.4 nm between the Gd nanoparticles, larger than that in the 5.5-nm-diam cluster, the 8-nm-diam Gd nanoparticle cluster should have weaker dipolar effects. However, there are two features which favor larger dipolar effects. The saturation magnetic moment of an 8-nm-diam Gd nanoparticle is  $6.11 \times 10^4 \mu_B$ , which is around three times larger than that of a 5.5-nm-diam Gd nanoparticle, which is  $1.98 \times 10^4 \mu_B$ . As a result, the magnetic field produced by an 8-nm-diam Gd nanoparticle is larger. For instance, at saturation ( $\langle \mu \rangle = \mu_0$ ) the magnetic field produced by an 8 nm diameter in the nearest Gd nanoparticle, at a distance  $d = 14.4$  nm, is  $2\mu_0/d^3 \approx 380$  Oe, which is slightly larger than the corresponding value in the 5.5-nm-diam Gd nanoparticle cluster (350 Oe).

The energy associated to the dipolar interaction of two nearest-neighbor Gd nanoparticles at saturation,  $E = 2\mu_0^2/d^3$ , may also be used to estimate and compare the dipolar energy effects. It corresponds to a temperature of 467.9 K for the 5.5-nm-diam Gd nanoparticle cluster, and a larger temperature of 1563.3 K for the 8-nm-diam Gd nanoparticle cluster.

Furthermore, the 8-nm-diam Gd cluster holds a larger number of nanoparticles than the 5.5-nm-diam Gd cluster.

#### D. 10.0-nm-diam Gd nanoparticle cluster

In Fig. 9 we show the thermal hysteresis loop of a 10-nm-diam Gd nanoparticle cluster, with an 846-nm major axis and a 186-nm minor axis, holding 1671 Gd nanoparticles distributed uniformly with a center-to-center distance of 22.0 nm, for an external field strength is 48.5 Oe.

Notice from Figs. 7 and 9 that the dipolar effects are much stronger in the 10-nm-diam Gd nanoparticle cluster than in the 8-nm-diam Gd nanoparticle cluster.

As shown in Fig. 7, for an external field strength of  $H = 88$  Oe, the 8-nm-diam nanoparticle cluster with center-to-center distance of 14.4 nm has a thermal loop width of  $\delta T = 750$  K,

which is smaller than the thermal loop width of the 10-nm-diam Gd nanoparticle cluster shown in Fig. 9.

As shown in Fig. 9, the thermal loop width of the 10-nm-diam Gd nanoparticle cluster, with an almost 53% larger center-to-center nanoparticle distance of 22 nm, for a smaller value of the external field strength,  $H = 48.5$  Oe, is  $\delta T = 836$  K.

It is instructive to compare the magnetic states along the corresponding cooling curves. In Fig. 10 we show the magnetization and dipolar field patterns along selected temperature values of the cooling and heating branches of the 846-nm major axis and 186-nm minor axis ellipsoidal clusters holding 1671 Gd nanoparticles, with 10 nm diameter, with a center-to-center distance of 22 nm, and for an external field strength of  $H = 48.5$  Oe.

As shown in Figs. 8(a1) and 8(a2), at 1000 K the 8-nm-diam Gd nanoparticle cluster has an average thermal value of the nanoparticle magnetic moments around  $\langle \mu \rangle \approx 0.62\mu_0$ , requiring an average dipolar field strength of  $H_d \approx 594$  Oe. At the same temperature, as shown in Figs. 10(a1) and 10(a2), the 10-nm-diam Gd nanoparticle cluster has a larger average thermal value of the nanoparticle magnetic moments  $\langle \mu \rangle \approx 0.66\mu_0$ , requiring a lower value of the average dipolar field strength,  $H_d \approx 348$  Oe. It sounds intuitive that to achieve thermal stabilization of the magnetic moments, the larger-diameter nanoparticle cluster should require lower values of the local field. This is confirmed at room temperature.

At room temperature the average thermal values in the 8-nm-diam Gd nanoparticle cluster, as shown in Figs. 8(b1) and 8(b2), are  $\langle \mu \rangle \approx 0.92\mu_0$  and  $H_d \approx 896$  Oe, while the 10-nm-diam Gd nanoparticle cluster requires a lower dipolar field strength,  $H_d \approx 494$  Oe, for a larger thermal average of the nanoparticle magnetic moments  $\langle \mu \rangle \approx 0.93\mu_0$  at room temperature, as shown in Figs. 10(b1) and 10(b2).

By further reduction of the temperature as shown in the two pairs of panels Figs. 10(c1) and 10(c2) and Figs. 10(d1) and 10(d2), the average thermal values of the nanoparticle magnetic moments and dipolar field increase to  $\langle \mu \rangle \approx 0.94\mu_0$  and  $H_d \approx 503$  Oe, at a temperature of 232 K, and  $\langle \mu \rangle \approx 0.95\mu_0$  and  $H_d \approx 563$  Oe, at a temperature of 210 K when the AFS forms. Notice that the corresponding thermal average values at the formation of the AFS at a temperature of 230 K in the 8-nm-diam Gd nanoparticle cluster has a similar value  $\langle \mu \rangle \approx 0.94\mu_0$  and requires a larger local field strength of  $H_d \approx 1.0$  kOe.

On the heating branch of the 10-nm-diam Gd nanoparticle cluster the AFS stays stable up to a temperature of 1024 K, as shown in Figs. 10(e1) and 10(e2), and at  $T = 1046$  K the thermal loop closes with the formation of the DSFS, as shown in Figs. 10(f1) and 10(f2), resulting in the thermal loop width of  $\delta T = 836$  K.

One might expect that the cluster magnetization should be a monotonically decreasing function of the temperature. Thus, reducing the temperature the magnetization should increase.

We have found that this is partially true in the thermal hysteresis loops of the Gd clusters that we have examined in this study, as shown for instance in Figs. 5, 7, and 9. Along the cooling branches of the thermal loops there is an initial temperature interval where the magnetization increases, as shown for instance in Fig. 9 from  $T = 1200$  K to  $T = 232$  K.

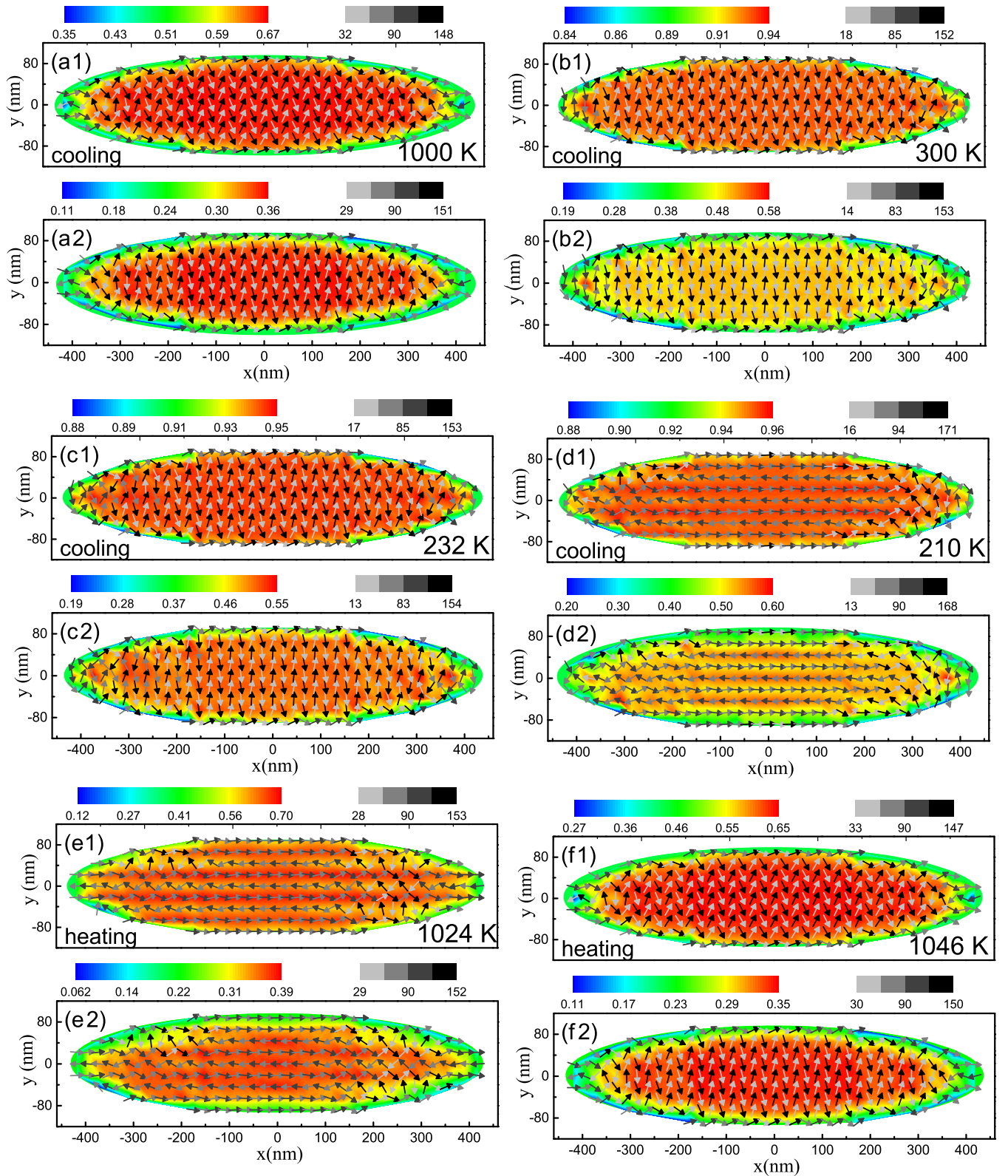


FIG. 10. Thermal average magnetic moment ( $\langle \mu \rangle / \mu_0$ ) (upper panels) and dipolar field patterns (lower panels) for selected temperature values, as indicated in Fig. 9, in the cooling or the heating branch of the thermal hysteresis loop for 846-nm major axis and 186-nm minor axis ellipsoidal clusters holding 1671 Gd nanoparticles, with 10 nm diameter, distributed uniformly with a center-to-center distance of 22 nm. The left-hand-side color bars show either the values of the fractional thermal average magnetic moment per Gd nanoparticle, or the strength of the dipolar field in units of kOe. The right-hand-side color bars show the out-of-plane angles ( $\theta$ ) of the nanoparticles magnetic moments or the dipolar field.

As shown in the three pairs of panels Figs. 10(a1) and 10(a2), Figs. 10(b1) and 10(b2), and Figs. 10(c1) and 10(c2), from  $T = 1000$  K to  $T = 232$  K the thermal average magnetic moment values increase, with values around  $\langle \mu \rangle \approx 0.66\mu_0$ , for  $T = 1000$  K,  $\langle \mu \rangle \approx 0.93\mu_0$  for  $T = 300$  K, and  $\langle \mu \rangle \approx 0.94\mu_0$  for  $T = 232$  K. The thermal average dipolar field strength increases also, with corresponding values of  $H_d \approx 0.348$ ,  $H_d \approx 0.494$ , and  $H_d \approx 0.503$  kOe. In this temperature range, the magnetization increases by pure thermal effects, but the magnetic phase does not change and corresponds to the DSFS.

However, the thermal loops shown in Figs. 5, 7, and 9, for ellipsoidal clusters holding Gd nanoparticles with diameters of 5.5, 8, and 10 nm, have an interesting feature. As seen in these figures, there is a magnetization drop at low temperature values. This is a signature of the transition from the DSFS to the AFS, which is a lower magnetization phase.

As shown in Fig. 9 and in the two pairs of panels in Figs. 10(c1) and 10(c2) and Figs. 10(d1) and 10(d2), from  $T = 232$  K to  $T = 210$  K there is an increase in the thermal average values of the Gd magnetic moments from  $\langle \mu \rangle \approx 0.94\mu_0$  to  $\langle \mu \rangle \approx 0.95\mu_0$ , with a corresponding increase of the thermal average dipolar field strength from  $H_d \approx 0.503$  to  $H_d \approx 0.563$  kOe. Thus, since the thermal average value of the magnetic moments increases in reducing the temperature from 232 to 210 K, one might expect that the magnetization should also increase. However, at the temperature of 210 K the magnetization drops. This reduction in the magnetization originates in a magnetic phase change from the DSFS to the AFS. Owing to the nucleation of the AFS in most of the cluster volume, as shown in Fig. 10(d1), with most nanoparticles with nearest-neighbor nanoparticles with the magnetic moment in the opposite direction, at 210 K the system has a smaller net magnetization.

We suggest that the transition from the DSFS to the AFS, by cooling the Gd cluster, with a reduction of the magnetization, is a key feature of the thermal hysteresis of superparamagnetic nanoparticle clusters and might be used to confirm that the dipolar interaction alone suffices to stabilize the magnetic order in these systems.

#### IV. CONCLUSIONS

In summary, we have discussed the impact of the dipolar interaction in the magnetic phases and the thermal hysteresis of ellipsoidal clusters holding superparamagnetic Gd nanoparticles.

We have assumed there is no interaction between the Gd nanoparticles, other than the long-range dipolar interaction. We have shown that for large Gd nanoparticle packing densities one may tailor the thermal loop width using modest external magnetic field strengths, smaller than 100 Oe, as shown in Table I and in Figs. 5, 7, and 9.

Our results indicate that, owing to the large magnetization of Gd, the dipolar interaction may lead to surprisingly large thermal average values of the nanoparticle's magnetic moments. For instance, above room temperature the average

dipolar field strength may reach a few hundred oersted and stabilize the magnetic moment values to large fractions of the saturation value.

The thermal hysteresis loop width may be tailored by choosing the Gd nanoparticle diameter and the cluster size. We have shown, for instance, that a 310.75-nm major axis and 66.55-nm minor axis ellipsoidal cluster of 5.5-nm-diam Gd nanoparticles holding 795 Gd nanoparticles distributed uniformly, with a center-to-center distance of 10.2 nm, exhibits a thermal loop width of  $\delta T = 88$  K for an external field strength of 85 Oe. We have also shown that a 10-nm-diam Gd cluster, with an 846-nm major axis and a 186-nm minor axis, holding 1671 Gd nanoparticles distributed uniformly with a center-to-center distance of 22.0 nm, exhibits a much wider thermal loop, with  $\delta T = 836$  K, for a smaller external field strength of 48.5 Oe.

We have also found, for the systems investigated in the present study, that for large values of the external field strength there is no thermal hysteresis, because the Zeeman energy inhibits the formation of the AFS.

In the 5.5-nm-diam Gd nanoparticle ellipsoidal cluster with a 310.75-nm major axis and 66.55-nm minor axis, holding 795 Gd nanoparticles with center-to-center distance of 10.2 nm, for an external field strength of 100 Oe the DSFS forms at 363 K, in the cooling branch, and stays stable down to low temperature values,  $T = 200$  K.

In the 8-nm-diam Gd nanoparticle cluster with a 555-nm major axis and a 123-nm minor axis, and in the 10-nm-diam Gd cluster, with an 846-nm major axis and a 186-nm minor axis, both holding 1671 Gd nanoparticles with a center-to-center distance of 14.4 and 22 nm, respectively, for an external field strength of 100 Oe, the DSFS forms at high temperatures ( $T \approx 1200$  K) and stays stable along the cooling curve until low temperature values ( $T = 200$  K).

In these cases, there is no thermal hysteresis. The sequence of states in the heating branch curve is equal to that in the cooling branch curve. We suggest that this might be a point of some interest in applications of superparamagnetic clusters.

Also, we have shown that the thermal hysteresis of large-eccentricity ellipsoidal clusters holding 5.5-, 8-, or 10-nm-diam Gd nanoparticles, originates in transitions from the DSFS to the AFS, in the cooling branch of the thermal loop, and transitions from the AFS to the DSFS in the heating branch.

These two states of superparamagnetic nanoparticle clusters are stabilized by the nanoparticle dipolar interaction [16]. Thus, we suggest that the study of thermal hysteresis might be used to confirm that the dipolar interaction may suffice to stabilize the magnetic order in superparamagnetic nanoparticle clusters.

#### ACKNOWLEDGMENTS

The authors acknowledge support from CNPq, CAPES, and FAPERJ. The work of A.S.C. and A.L.D. was supported by CNPq Grants No. 350773 and No. 309676.

- [1] T. Kim, S. Lim, J. Hong, S. G. Kwon, J. Okamoto, Z. Y. Chen, J. Jeong, S. Kang, J. C. Leiner, J. T. Lim, C. S. Kim, D. J. Huang, T. Hyeon, S. Lee, and J.-G. Park, *Sci. Rep.* **8**, 5092 (2018).
- [2] S. Demirtas, R. E. Camley, and A. R. Koymen, *Appl. Phys. Lett.* **87**, 202111 (2005).
- [3] R. E. Camley, W. Lohstrohb, G. P. Felcher, N. Hosoitod, and H. Hashizume, *J. Magn. Magn. Mater.* **286**, 65 (2005).
- [4] S. Demirtas, M. R. Hossu, R. E. Camley, H. C. Mireles, and A. R. Koymen, *Phys. Rev. B* **72**, 184433 (2005).
- [5] M. R. Hossu, Y. Hao, and A. R. Koymen, *J. Phys.: Condens. Matter* **20**, 215224 (2008).
- [6] J. P. Andrés, J. A. Gonzalez, T. P. A. Hase, B. K. Tanner, and J. M. Riveiro, *Phys. Rev. B* **77**, 144407 (2008).
- [7] A. L. Dantas, R. E. Camley, and A. S. Carriço, *IEEE Trans. Magn.* **42**, 2942 (2006).
- [8] A. L. Dantas, R. E. Camley, and A. S. Carriço, *Phys. Rev. B* **75**, 094436 (2007).
- [9] A. L. Dantas, A. S. W. T. Silva, G. O. G. Rebouças, A. S. Carriço, and R. E. Camley, *J. Appl. Phys.* **102**, 123907 (2007).
- [10] F. I. F. Nascimento, A. L. Dantas, L. L. Oliveira, V. D. Mello, R. E. Camley, and A. S. Carriço, *Phys. Rev. B* **80**, 144407 (2009).
- [11] W. D. Corner, W. C. Roe, and K. N. R. Taylor, *Proc. Phys. Soc.* **80**, 927 (1962).
- [12] C. L. Dennis, A. J. Jackson, J. A. Borchers, R. Ivkov, A. R. Foreman, J. W. Lau, E. Goernitz, and C. Grüttner, *J. Appl. Phys.* **103**, 07A319 (2008).
- [13] C. L. Dennis, A. J. Jackson, J. A. Borchers, P. J. Hoopes, R. Strawbridge, A. R. Foreman, J. van Lierop, C. Grüttner, and R. Ivkov, *Nanotechnology* **20**, 395103 (2009).
- [14] S. Bedanta, O. Petracic, and W. Kleemann, in *Handbook of Magnetic Materials*, edited by K. J. H. Buschow (Elsevier, New York, 2015), Vol. 23.
- [15] S. Bedanta, T. Seki, H. Iwama, T. Shima, and K. Takanashi, *Appl. Phys. Lett.* **107**, 152410 (2015).
- [16] S. S. Pedrosa, S. M. S. B. Martins, Jr., R. M. Souza, J. T. S. Dantas, C. M. Souza, G. O. G. Rebouças, J. M. de Araújo, A. L. Dantas, and A. S. Carriço, *Appl. Phys.* **123**, 233902 (2018).
- [17] D. A. Venero, S. E. Rogers, S. Langridge, J. Alonso, M. L. Fdez-Gubieda, A. Svalov, L. F. Barquin, *J. Appl. Phys.* **119**, 143902 (2016).
- [18] M. S. Andersson, J. A. De Toro, S. S. Lee, P. S. Normile, P. Nordblad, and R. Mathieu, *Phys. Rev. B* **93**, 054407 (2016).
- [19] D. S. Schmool and H. Kachkachi, *Solid State Phys.* **67**, 1 (2016).
- [20] A. Sugawara and M. R. Scheinfein, *Phys. Rev. B* **56**, R8499 (1997).
- [21] A. Sugawara, *IEEE Trans. Magn.* **37**, 2123 (2001).
- [22] D. X. Chen, A. Sanchez, H. Xu, H. Gu, and D. Shi, *J. Appl. Phys.* **104**, 093902 (2008).
- [23] M. E. Materia, P. Guardia, A. Sathya, M. P. Leal, R. Marotta, R. Di Corato, and T. Pellegrino, *Langmuir* **31**, 808 (2015).
- [24] M. Cyrot *et al.*, in *Magnetism Fundamentals*, edited by E. du Trémolet de Lacheisserie, D. Gignoux, and M. Schlenker (Springer, Boston, 2005), p. 501.